ChemComm

Cite this: *Chem. Commun.*, 2012, **48**, 5656–5658

www.rsc.org/chemcomm

COMMUNICATION

Syntheses and magnetic properties of Cr_2Te_3 and $CuCr_2Te_4$ nanocrystals†

Karthik Ramasamy, Dipanjan Mazumdar, Robert D. Bennett and Arunava Gupta*

Received 20th March 2012, Accepted 16th April 2012
DOI: 10.1039/c2cc32021e

The Cr-based tellurides are attractive material systems for fundamental studies and potential applications. Colloidal syntheses of ferromagnetic Cr_2Te_3 and $CuCr_2Te_4$ nanocrystals with uniform morphology and narrow size distribution are reported together with their detailed magnetic characterisation.

Nanoscale magnetic materials are being intensively investigated because of both their unique properties and potential applicability in different fields, including spin-based electronics, recording media, magneto-optics, magneto-caloric refrigeration, biomedical imaging, *etc*.[1] Chromium-based tellurides in the bulk are known to be ferromagnetic with variable Curie temperatures (T_Cs). Chromium telluride itself exists in various stoichiometries, including $Cr_{1-x}Te$, Cr_2Te_3, Cr_3Te_4, Cr_5Te_8 and Cr_5Te_6. All these compositions crystallize in the hexagonal NiAs-type structure with ordered Cr vacancies.[2] Ferromagnetism in these compounds, with T_Cs ranging from 180 to 340 K, results primarily from ordering of the magnetic moment localized at the Cr sites.[3] Because of its unusual magnetic properties, metallic Cr_2Te_3 ($T_C \sim 180$ K) is one of the better studied systems in this family,[4] but a detailed understanding of its complex magnetic structure is still lacking.

Ferromagnetic ordering also occurs in a remarkable class of Cr-based chalcogenide spinels (chalcospinels) that display metallic, semiconducting, or insulating characteristics.[5] In particular, the compounds $CuCr_2S_4$, $CuCr_2Se_4$ and $CuCr_2Te_4$ are metallic with T_Cs of 377, 430 and 360 K, respectively.[6] Because of their high Curie temperatures, these materials are potential candidates for spin-based electronics and other applications. Furthermore, recent band structure calculations suggest the exciting possibility of inducing half-metallicity, *i.e*., a material in which there is a gap in one spin band at the Fermi level and no gap in the other spin band, in some of the mixed Cu,Cd chalcospinels.[7] Thus far only a few tellurospinels (MCr_2Te_4, M = Cu, Ag, Fe) have been identified, among them the Cu and Ag analogues are reported to be ferromagnetic at room temperature.[8] Thus, metallic behavior and ferromagnetism with T_C above room temperature are the significant characteristics of $CuCr_2Te_4$. The material has also been reported to exhibit a pronounced room temperature magneto-optical Kerr effect.[9]

Unlike other semiconducting and metallic tellurides, the synthesis of Cr-based tellurides is limited. Conventional solid state methods have been developed for the bulk synthesis of Cr_2Te_3 and $CuCr_2Te_4$ using elemental precursors.[4,10] However, solution-based synthesis of these compounds in any form (either bulk or nano-sized) remains largely unexplored. This can be attributed in part to difficulties in controlling the oxidation state of chromium and limited known Te precursors for phase selective synthesis of Cr_2Te_3 and $CuCr_2Te_4$. The utility of these unique materials can undoubtedly be augmented if they can be synthesized with highly controlled dimensions, such as colloidal nanocrystals. We recently reported chemical routes for the synthesis of phase-pure $CuCr_2S_4$ and $CuCr_2Se_4$ nanocrystals.[11] Building on our experience with solution-phase synthesis of these magnetic chalcospinels, herein we report the first colloidal syntheses of Cr_2Te_3 and $CuCr_2Te_4$ nanocrystals. The syntheses involve reduction of tellurium with sodium borohydride in boiling trioctylamine to produce telluride ions, followed by reaction with chloride salts of the cation(s).

For the synthesis of Cr_2Te_3 nanocrystals, 0.4 mmol of Te powder and 0.4 mmol of $NaBH_4$ in 25 mL of TOA (98%) were heated to 170–180 °C under vacuum and then to 350–355 °C under N_2, and maintained at this temperature for 1 h. In another vessel, 0.4 mmol of $CrCl_3{\cdot}6H_2O$ and 2 mL of oleylamine (OLA) were placed under vacuum for 10 min and then in a N_2 atmosphere for 10 min at room temperature. The vessel was heated in stages to 80–90 °C under vacuum and then to 180–190 °C under N_2. The $CrCl_3{\cdot}6H_2O$ and oleylamine mixture was then rapidly injected into the Te-containing vessel. The vessel was then quickly reheated to the original temperature (350–355 °C), and the resulting mixture continually stirred for 30 min. Following this, the mixture was cooled to 60–70 °C and a 1 : 3 mixture of hexane and ethanol was added to precipitate the nanocrystals. A similar procedure was used for the synthesis of $CuCr_2Te_4$ nanocrystals but using excess of tellurium powder (0.8 mmol) and $NaBH_4$ (0.8 mmol), and a mixture of $CuCl_2$ and $CrCl_3{\cdot}6H_2O$ (with 1 : 2 stoichiometry of Cu : Cr) in oleylamine was injected into the Te-containing vessel.

Center for Materials for Information Technology, University of Alabama, Tuscaloosa, Alabama 35487, USA. E-mail: agupta@mint.ua.edu; Fax: +1 205-348-2346; Tel: +1 205-348-3822

† Electronic supplementary information (ESI) available: Reaction schemes; TEM, EDX images; Raman spectra; isothermal and Arrott plots. See DOI: 10.1039/c2cc32021e

We also investigated the use of other commonly used tellurium precursors, such as trioctylphosphine telluride (TOP-Te) and diphenyl ditelluride (DPDT). The formation of a Cr-coordination complex with excess phosphine was observed in the experiment carried out using TOP-Te, while a large amount of elemental tellurium was isolated using DPDT. We further established that a temperature range of 180–190 °C for the Cr–OLA or CuCr–OLA mixture before injection was crucial for obtaining the desired products. The formation of an alkylammonium selenide complex was previously noted during reduction of selenium with $NaBH_4$ in hydrophobic alkylamines.[12] Based on this result, we envision the formation of a trioctylammonium telluride complex in our method of synthesis when the tellurium is refluxed with $NaBH_4$ in trioctylamine. A possible sequence of reactions in the syntheses of Cr_2Te_3 and $CuCr_2Te_4$ nanocrystals is given in Schemes S1 and S2 (ESI†).

X-ray diffraction (XRD) measurements confirm the phase purity of the as-synthesized Cr_2Te_3 nanocrystals, as shown in Fig. 1a, and the diffraction pattern matches very well with the NiAs-type hexagonal structure with the $P\bar{3}1c$ (163) space group (shown in the Fig. 1a inset). The diffraction peaks are indexed as the (112), (114), (300), (116) and (222) planes of the hexagonal Cr_2Te_3 phase (ICDD no. 029–0458). Based on the peak positions the estimated lattice parameters are a = 6.82 Å and c = 12.08 Å, which are consistent with the values reported for bulk Cr_2Te_3.[13] Furthermore, the XRD pattern rules out the presence of other known chromium telluride phases or impurities. The transmission electron microscopy (TEM) image in Fig. 1b shows oval-shaped Cr_2Te_3 spheroid nanocrystals with an average length of 12 ± 2 nm, which is in agreement with the particle size (14 nm) estimated from the width of the (112) peak using the Scherrer equation. The high-resolution TEM (HRTEM) image in Fig. 1c shows lattice fringes with measured d spacing of 0.29 nm, corresponding to the (112) reflection of hexagonal Cr_2Te_3. The bright spots seen in the fast Fourier transform (FFT) pattern (Fig. 1c inset) can be indexed to the (112) planes. Energy dispersive X-ray spectroscopy (EDX) measurements confirm the Cr/Te ratio to be close to 2 : 3.

The structure of solution-synthesized $CuCr_2Te_4$ nanocrystals has also been confirmed by XRD analysis. The XRD pattern in Fig. 2a shows diffraction peaks corresponding primarily to

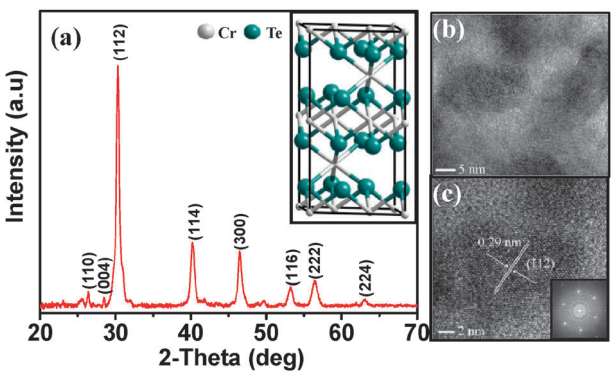

Fig. 1 (a) XRD pattern of Cr_2Te_3 nanocrystals. Inset shows the crystal structure of Cr_2Te_3. (b) TEM image of Cr_2Te_3 nanocrystals. (c) HRTEM image of a typical Cr_2Te_3 nanocrystal. Inset shows the fast Fourier transform (FFT) image extracted from image (c).

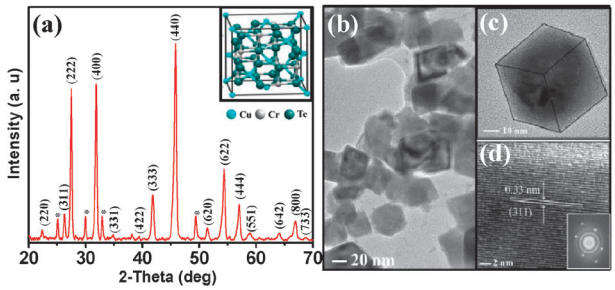

Fig. 2 (a) XRD patterns of $CuCr_2Te_4$ spinel nanocrystals. Inset shows crystal structure of $CuCr_2Te_4$. (b) and (c) TEM images of $CuCr_2Te_4$ nanocrystals. (d) HRTEM image of a $CuCr_2Te_4$ nanocrystal. Inset of panel (d) shows the FFT image extracted from image (d).

the cubic spinel $CuCr_2Te_4$ phase, along with small amounts of $Cu_{3-x}Te_2$ and Cr_2Te_3 impurity phases. The Cr_2Te_3 impurity phase has also been observed in conventional solid state synthesis.[10] Besides phase stability, one of the main difficulties involved in the synthesis of phase-pure $CuCr_2Te_4$ nanocrystals is the lack of high temperature (> 360 °C) coordinating agents or solvents. The major diffraction peaks in Fig. 2a are indexed as (222), (400), (333), (440), (622) and (444) reflections of the spinel $CuCr_2Te_4$ phase (fcc, space group $Fd3m$) that can be matched with ICDD pattern no. 058–0254 (crystal structure shown in the Fig 2 inset). The calculated lattice parameter a = 11.19 Å is in agreement with that observed for bulk $CuCr_2Te_4$ (11.13 Å).[10] An average particle size of 21.1 nm is estimated from the width of the (440) peak using the Scherrer equation. This is comparable with the size measured using TEM. Fig. 2b and c show TEM images with close to perfect cube-shaped particles with an average size of 23 ± 2 nm. The lattice fringe spacing seen in the HRTEM image (Fig. 2d) is 0.33 nm, which corresponds to the distance between (311) planes of spinel $CuCr_2Te_4$. EDX analysis of the nanocrystals provides a Cu/Cr/Te ratio of 1 : 2 : 4.4. There is no evidence of the presence of other possible impurities, such as sodium, chlorine or boron (Fig. S2, ESI†).

The Raman spectra of $CuCr_2Te_4$ nanocrystals (excitation at 633 nm) in Fig. S3a (ESI†) show three major peaks at 103, 123, 160 cm^{-1}, corresponding to the F_{2g}, E_g, F_{2g} modes of the spinel structure. Fig. S3b (ESI†) illustrates the atomic displacements corresponding to the different Raman modes, with the F_{2g}, E_g, F_{2g} modes corresponding to Cu-translation, Te–Cu–Te bending and Cu-translation against Te, respectively.

We analyzed the magnetic properties of the Cr_2Te_3 and $CuCr_2Te_4$ nanocrystals using a SQUID magnetometer in order to determine the Curie temperature and saturation magnetization. Field-cooled (FC) and zero-field-cooled (ZFC) measurements of the nanocrystals, with the applied magnetic field of 100 Oe and 50 Oe, are shown in Fig. S4a and b (ESI†). Low-field (50 Oe) measurements on Cr_2Te_3 and $CuCr_2Te_4$ nanocrystals provide Curie temperatures (T_Cs) of ~190 K and ~330 K respectively. The measured T_Cs for both nanocrystals are in good agreement with reported bulk values (~183 K for Cr_2Te_3; ~326 K for $CuCr_2Te_4$).[4,10] Magnetization measurements as a function of magnetic field for the Cr_2Te_3 nanocrystals show superparamagnetic (SP) behavior at 180 K and ferromagnetic behavior at 5 K (Fig. 3a). It is interesting to

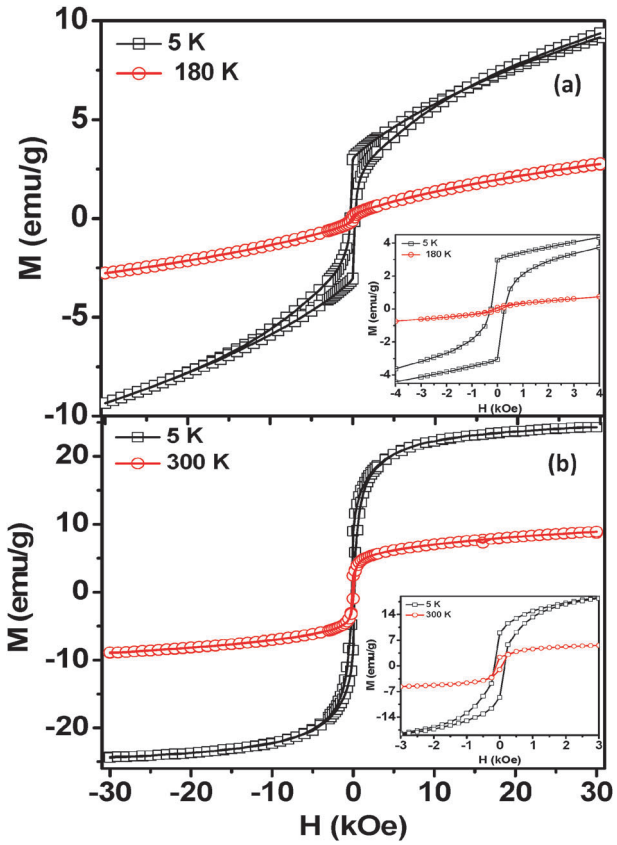

Fig. 3 Magnetization (M) as a function of applied field (H) measurements for (a) Cr_2Te_3 at 5 K and 180 K; (b) $CuCr_2Te_4$ at 5 K and 300 K. Enlarged portions showing the coercivity (insets of (a) and (b)).

note that a sharp switching is observed at 5 K with low coercivity ($H_C \sim 270$ Oe) and a remanent magnetization of 2.93 emu g^{-1}, but the magnetization does not saturate even at 3 Tesla. Non-saturation of magnetization even at high magnetic fields has also been observed in bulk samples, for which the T_C and magnetization also decrease with applied pressure.[4] These unusual characteristics have been attributed to noncollinear spin ordering likely originating from near-degeneracy of ferromagnetic and ferrimagnetic alignment in the Cr-deficient layer.[4a] Measurements on $CuCr_2Te_4$ nanocrystals indicate ferromagnetic and near-superparamagnetic behavior at 5 K and 300 K, respectively (Fig. 3b). Unlike Cr_2Te_3, a saturated hysteresis loop is obtained at 5 K for $CuCr_2Te_4$ with a saturation magnetization value of 24 emu g^{-1} (2.95 μ_B f.u.$^{-1}$). Moreover, a relatively low H_C value of $\sim$165 Oe, indicative of a soft ferromagnet, and a remanent magnetization of $\sim$8.9 emu g^{-1} are observed. The measured magnetization values for both nanocrystals are lower than their bulk counterparts ($\sim$5 μ_B f.u^{-1} for both Cr_2Te_3 (at 10 Tesla) and $CuCr_2Te_4$).[4,10] This decrease is not unexpected since with reduced dimensions of nanoscale materials the number surface atoms increases, which introduces surface disorder, defects, dangling bonds and vacancies at anion and/or cation sites. These effects will significantly reduce the number of spins, leading to a decrease in the net magnetization.[14] We have also measured the isothermal magnetization at temperatures around T_C for both nanocrystals and the results are shown in Fig. S5a and S6a (ESI†). The Arrott plots near the transition temperatures for Cr_2Te_3 and $CuCr_2Te_4$ nanocrystals show nonlinearity with downward curvature. The observed nonlinearity likely represents deviation from the Landau model for both these systems.[10b]

In summary, we have synthesized nanocrystals of Cr_2Te_3 and $CuCr_2Te_4$ by reduction of tellurium with sodium borohydride in boiling trioctylamine to produce telluride ions, followed by reaction with chloride salts of the cations. The synthesis yields oval-shaped hexagonal Cr_2Te_3 and cube-shaped spinel $CuCr_2Te_4$ nanocrystals. Magnetic measurements indicate Curie temperature (T_C) of $\sim$190 K and $\sim$330 K for Cr_2Te_3 and $CuCr_2Te_4$ nanocrystals, respectively. Nanocrystals of both the tellurides exhibit ferromagnetic behavior at low temperatures. For Cr_2Te_3 the magnetization at 5 K does not saturate even with a magnetic field of 3 Tesla, while $CuCr_2Te_4$ yields a saturation magnetization (M_S) value of 24 emu g^{-1} (2.95 μ_B f.u.$^{-1}$). A detailed investigation of the syntheses and magnetic properties of Cr_2Te_3 and $CuCr_2Te_4$ nanocrystals with different size and shape is underway and will be reported elsewhere.

This work is supported by the National Science Foundation under Grant No. CHE-1012850. The authors are grateful to Dr Vladimir Kuznetsov at Oxford University for the Rietveld refinement and Dr Shane Street at the University of Alabama for the Raman measurements.

Notes and references

1 (*a*) S. Si, A. Kotal, T. K. Mandal, S. Giri, H. Nakamura and T. Kohara, *Chem. Mater.*, 2004, **16**, 3489; (*b*) S. H. Sun, C. B. Murray, D. Weller, L. Folks and A. Moser, *Science*, 2000, **87**, 1989; (*c*) H. Zeng, J. Li, J. P. Liu, Z. L. Wang and S. H. Sun, *Nature*, 2002, **420**, 395.
2 H. Ipser, K. L. Komarek and K. O. Klepp, *J. Less-Common Met.*, 1983, **92**, 265.
3 J. Wontcheu, W. Bensch, S. Mankovsky, S. Polesya and H. Ebert, *Prog. Solid State Chem.*, 2009, **37**, 226.
4 (*a*) S. J. Youn, S. K. Kwon and B. I. Min, *J. Appl. Phys.*, 2007, **101**, 09G522; (*b*) T. Kanomata, Y. Sugawara, K. Kamishima, H. Mitamura, T. Goto, S. Ohta and T. Kaneko, *J. Magn. Magn. Mater.*, 1998, **177**, 589; (*c*) J. Dijkstra, H. H. Weitering, C. F. Van Bruggen, C. Haas and R. A. De Groot, *J. Phys.: Condens. Matter*, 1989, **1**, 9141; (*d*) M. Yuzuri, T. Kanomata and T. Kaneko, *J. Magn. Magn. Mater*, 1987, **70**, 223.
5 F. K. Lotgering, *Solid State Commun.*, 1964, **2**, 55.
6 (*a*) J. B. Goodenough, *Solid State Commun.*, 1967, **5**, 577; (*b*) P. K. Baltzer, H. W. Lehmann and Robbins, *Phys. Rev. Lett.*, 1965, **15**, 493.
7 Y.-H. A. Wang, A. Gupta, M. Chshiev and W. H. Butler, *Appl. Phys. Lett.*, 2009, **94**, 062515.
8 A. Payer, A. Kamlowski and R. Schollhorn, *J. Alloys Compd.*, 1992, **185**, 89.
9 F. K. Lotgering and G. H. A. M. Van der Steen, *Solid State Commun.*, 1971, **9**, 1741.
10 (*a*) T. Suzuyama, J. Awaka, H. Yamamoto, S. Ebisu, M. Ito, T. Suzuki, T. Nakama, K. Yagasaki and S. J. Nagata, *Solid State Chem.*, 2006, **179**, 140; (*b*) R. Li, C. Zhang and Y. Zhang, *Solid State Commun.*, 2012, **152**, 173.
11 (*a*) K. Ramasamy, D. Mazumdar, Z. Zhou, Y.-H. A. Wang and A. Gupta, *J. Am. Chem. Soc.*, 2011, **133**, 20716; (*b*) Y.-H. A. Wang, N. Bao, L. Shen, P. Padhan and A. Gupta, *J. Am. Chem. Soc.*, 2007, **129**, 12408.
12 S. C. Riha, B. A. Parkinson and A. L. Prieto, *J. Am. Chem. Soc.*, 2011, **133**, 15272.
13 T. Hamasaki, T. Hashimoto, Y. Yamaguchi and H. Watanabe, *Solid State Commun.*, 1975, **16**, 895.
14 D. Caruntu, G. Caruntu and C. J. O'Connor, *J. Phys. D: Appl. Phys.*, 2007, **40**, 5801.

